PROJECT TUBEFLIGHT

WILLIAM D. ERNST

LINEARIZED FLOW IN A CYLINDRICAL CAVITY

TR PT 6902

LINEARIZED FLOW IN A CYLINDRICAL CAVITY

by
William D. Ernst

This work was supported by the National Science Foundation under Grant No. NSF-GK-618 and by a National Aeronautics and Space Administration Fellowship, and constitutes part of a thesis submitted to the faculty of the School of Engineering in partial fulfillment of the requirements for the degree of Doctor of Philosophy.

RENSSELAER POLYTECHNIC INSTITUTE
TROY, NEW YORK

JANUARY, 1969

ACKNOWLEDGMENT

The author wishes to express his appreciation and gratitude to Dr. H. J. Hagerup for suggesting the problem and providing advice and guidance throughout the work.

SUMMARY

This third paper concludes an analysis of the laminar, large Reynolds number, two-dimensional recirculatory flow induced in a circular cylinder by the steady tangential motion of a segment of the periphery. In the first paper, the flow is shown to be dependent upon a thin, peripheral boundary layer. For this, a solution is derived from a Fredholm integral equation based on a linearized form of the von Mises equation. This linearized solution is obtained as a functional dependent upon a stretching function, and a primitive assumption for the value of this function is shown to yield a qualitatively correct solution. In the second paper, a nonlinear differential equation for the stretching function is derived for a class of boundary layer problems characterized by having a nonuniform initial velocity distribution, a constant free stream velocity, and a piecewise constant slip velocity at the wall. For a special case of this general problem, the stretching function is obtained, and the corresponding approximate solution is shown to be in good agreement with a previously unpublished exact solution. The present paper extends and combines the results of the two previous papers to obtain the approximate solution for the peripheral boundary layer in a circular cylinder. This solution is shown to satisfy an exact criterion, and the predicted flow pattern is discussed in some detail.

TABLE OF CONTENTS

LIST OF SYMBOLS

a	length of moving segment of S_b in physical plane
$\hat{a}$	length of moving segment of S_b in $\hat{x}_m$ plane
c	length of stationary segment of S_b in physical plane
$\hat{c}$	length of stationary segment of S_b in $\hat{x}_s$ plane
F	force on S_b
$g(x)$	$g(x) = \hat{x}$, coordinate transformation for von Mises stretching function
$k(x)$	von Mises stretching function
K	$K = U_c/U$, core velocity ratio
S_b	outermost closed streamline of recirculation flow field
u	velocity parallel to wall
$\tilde{u}$	transformed approximate solution to von Mises equation
$\hat{u}$	approximate solution to von Mises equation
U	constant velocity of moving segment of S_b
U_c	constant velocity at outer edge of boundary layer
x	distance measured parallel to wall in physical plane
$\hat{x}$	$\hat{x} = \int_0^x 1/k(\rho)\,d\rho$, distance parallel to wall in transformed plane
y	distance measured normal to wall
$\epsilon(x)$	von Mises stretching function
ρ	density
ν	kinematic viscosity
λ	$\lambda = c/a$, wall length ratio
ψ	$\psi = \partial u/\partial y$, stream function

Subscripts

m	refers to moving wall
s	refers to stationary wall

INTRODUCTION

In a previous paper,[1] an investigation was made of the laminar, large Reynolds number, two-dimensional recirculatory flow induced in a circular cylinder by the steady tangential motion of a segment of the periphery. The flow configuration was assumed to consist of a centered, constant-vorticity core surrounded by a thin, peripheral boundary layer (BL). A solution for this BL was derived from a Fredholm integral equation by the use of a linearized form of the von Mises BL equation. This form was obtained by replacing the nonlinear (in the von Mises equation) viscous term, $uu_{\psi\psi}$, by the term $k^{-1}(x)\, u_{\psi\psi}$. Since the function $k(x)$ may, for algebraic convenience, be incorporated in a transformation that stretches the local x coordinate, $k(x)$ is denoted as the von Mises stretching function. The linearized solution for the BL velocity distribution was obtained as a functional involving the stretching function. The explicit solution, denoted as the stretching function linearization (SFL) solution, can be derived from the linearized solution only upon the determination of the stretching function. Because the emphasis in reference 1 was placed on obtaining both a physical understanding of the flow field and a general linearized formulation, the stretching functions were not determined, and instead a very primitive assumption was made for their value in order to derive a qualitatively correct solution.

In a second paper,[2] both a linearized solution and a differential equation for the stretching function were derived for a certain general type of BL problems, characterized by having a nonuniform initial velocity distribution (NUIV), a constant free stream velocity, and a piecewise constant slip velocity at the wall. SFL solutions were in fact determined using both the Prandtl and the von Mises form of the BL equations, but

as explained in reference 2 the von Mises form is better for some NUIV problems, and will be used in the present paper. The auxiliary equation for k(x) is based on the following condition: at any x, the mean difference between the exact and linearized form of the BL equation, when evaluated using the linearized solution, must be zero. In reference 2, the SFL solution was derived for the simpler problems of a uniform initial velocity (UIV) distribution. The UIV problem, unlike the NUIV problem, has an exact solution. For the UIV case, the SFL solution and the exact solution were shown to be in satisfactory agreement for both the wall shear stress and typical velocity profiles.

The present paper extends and combines the results of the two previous papers to obtain an SFL solution, based on the von Mises equation, for the peripheral BL in a cylindrical flow field. This solution is shown to be in good agreement with a criterion for the velocity at the outer edge of the BL derived by Wood[3] from the exact equations. Based on this agreement it would seem that the SFL technique may with confidence be applied to more general BL problems.

THE STRETCHING FUNCTION LINEARIZATION TECHNIQUE

Solution of the Linearized von Mises BL Equation

The flow configuration on which the analysis is based is sketched below.

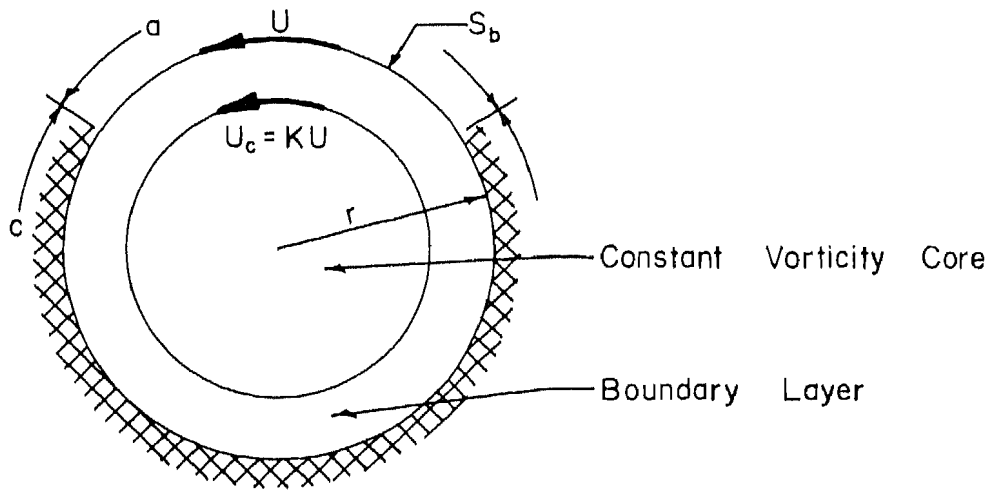

Fig. 1.

The bounding streamline of the flow field, S_b, is fixed, and the steady, two-dimensional recirculatory flow field is contained within an infinite circular cylinder of radius r. A segment of the periphery, of length a, is moving tangentially at the velocity U, and the remainder of the periphery, of length c, is a solid stationary wall. If the Reynolds number is

large enough, the flow pattern will be characterized by a thin boundary layer along the walls, and a central rotating core. In the analysis, it is assumed that the core is concentric to the cylinder, has constant vorticity, and has a tangential velocity of KU at its edge. From these assumptions, it follows that the thin, peripheral BL is the same as that on a flat wall in a free stream of constant velocity KU, and with boundary conditions at the wall of zero slip velocity and constant slip velocity, U, for the wall segments of length c and a, respectively. The wall segment length ratio is denoted by $\lambda = c/a$.

The basis of the analysis in reference 1 is the linearized von Mises BL equation which is given in nondimensional form by

$$k_{m,s}(x)\frac{\partial \tilde{u}^2_{m,s}}{\partial x} = \frac{\partial^2 \tilde{u}^2_{m,s}}{\partial \psi^2} \tag{1}$$

where the subscripts m and s refer to the moving and stationary segments, $\tilde{u}(x, \psi)$ is the velocity along a streamline, x is the distance from the leading edge of the segment, $\psi = \int u\, dy$ is the stream function, and k(x) is the stretching function. The boundary conditions for this equation are

$$\begin{aligned} &\tilde{u}_m(x,0) = 1, \quad \tilde{u}_s(x,0) = 0 \\ &\lim_{\psi\to\infty} \tilde{u}_m(x,\psi) = K, \quad \lim_{\psi\to\infty} \tilde{u}_s(x,\psi) = K \end{aligned} \tag{2}$$

After the coordinate transformation

$$\hat{x}_{m,s} = \int_0^x \frac{dp}{k_{m,s}(p)} = g_{m,s}(x) \tag{3}$$

$$\hat{u}_{m,s}(\hat{x}_{m,s}\,\psi) = \hat{u}_{m,s}(g_{m,s}(x), \psi) = \tilde{u}(x,\psi) \tag{4}$$

the solution of equation 1 with the above initial and boundary conditions, as derived in reference 1, can be expressed in the form

$$\hat{u}_m^2(\hat{x}_m, \psi) = \sum_{n=1}^{p} \{\theta((n-1)\hat{t} + \hat{c} + \hat{x}_m) - \theta(n\hat{t} + \hat{x}_m)\} + 1 - \theta(\hat{x}_m) + K^2\theta(p\hat{t} + \hat{c} + \hat{x}_m) \tag{5a}$$

$$\hat{u}_s^2(\hat{x}_s, \psi) = \sum_{n=1}^{p} \{\theta((n-1)\hat{t} + \hat{x}_s) - \theta((n-1)\hat{t} + \hat{a} + \hat{x}_s)\} + K^2\theta(p\hat{t} + \hat{x}_s) \tag{5b}$$

where p denotes the order of the solution for the initial velocity distribution, and

$$\begin{aligned} \hat{a} &= g_m(a) \\ \hat{c} &= g_s(c) \\ \hat{t} &= \hat{a} + \hat{c} \\ \theta(n) &= \operatorname{erf}\left(\frac{\psi}{2}\sqrt{\frac{1}{n}}\right) \end{aligned} \tag{5c}$$

The core velocity ratio, K, is unknown and must be determined from an additional physical constraint. Since the net torque on the flow field must be zero for steady state conditions, the integral of the shear stress over S_b is zero. Thus, K must satisfy the constraint $F_m + F_s = 0$, where

$$F_m = \frac{1}{2}\int_0^a \frac{\partial}{\partial y}\hat{u}_m^2(g_m(x), \psi)_{\psi=0}\,dx$$

$$F_s = \frac{1}{2}\int_0^c \frac{\partial}{\partial y}\hat{u}_s^2(g_s(x), \psi)_{\psi=0}\,dx \tag{6a,b}$$

The core velocity ratio, K, is a prime result of the analysis and will be used to support its validity.

The result given by equation 5a,b is of no value unless $g_{m,s}$ is available to make the transformation back to the physical plane through equations 3 and 4. The remaining objective of the analysis at this point, therefore, is simply to determine the stretching function $k_{m,s}$.

The Stretching Function

In reference 2, it is shown that the stretching function for the von Mises BL equation is

$$k_{m,s} \equiv \frac{\int_0^\infty \hat{u}_{m,s}^{-1} \frac{\partial \hat{u}_{m,s}^2}{\partial \hat{x}_{m,s}} d\psi}{\int_0^\infty \frac{\partial \hat{u}_{m,s}^2}{\partial \hat{x}_{m,s}} d\psi} \tag{7}$$

If the linearized solution given by equation 5a,b in terms of the stretched x coordinate is substituted into the expression on the right side of equation 7, and the integration is performed, then it is easily seen that the resulting expression will be a function of $\hat{x}_{m,s}$, $\hat{a}$, and $\hat{c}$. If this function of $\hat{x}_{m,s}$, $\hat{a}$, and $\hat{c}$ is denoted as $\epsilon_{m,s}(\hat{x}_{m,s}, \hat{a}, \hat{c})$, then it follows finally from equation 3 that the stretching function re-expressed in terms of the original x coordinate is

$$k_{m,s}(x) = \epsilon_{m,s}\left(g_{m,s}(x), g_m(a), g_s(c)\right) \tag{8a}$$

or

$$k_{m,s}(x) = \epsilon_{m,s}\left(\int_0^x \frac{d\rho}{k_{m,s}(\rho)}, \int_0^a \frac{d\rho}{k_m(\rho)}, \int_0^c \frac{d\rho}{k_s(\rho)}\right) \tag{8b}$$

A valuable result concerning k may be obtained by noting that $g'_{m,s} = 1/k_{m,s}$, and substituting this identity in equation 8a to yield

$$g'_{m,s} = 1/\epsilon_{m,s}\left(g_{m,s}(x), g_m(a), g_s(c)\right)$$

This first order nonlinear ordinary differential equation will yield a unique solution for $g_{m,s}$ provided $1/\epsilon_{m,s}$ is continuous and satisfies the Lipschitz condition. Thus for $g'_{m,s} \neq 0$, any $k_{m,s}$ determined as a solution of equation 8a, numerically or otherwise, will be unique. With

this result, the SFL solution of the exact, second order, nonlinear BL equation, may be obtained by solving first a second order linear partial differential equation which determines the functional form of ϵ , and then solving a first order nonlinear ordinary differential equation which determines k.

Thus, we are in a position to determine the BL flow field in the cylindrical cavity. The solutions of equation 8a for the stretching function, of equations 6a,b for the core velocity ratio, and of equations 3 and 5a,b for the velocity distribution are determined numerically. A synopsis of this procedure is given in Appendix I.

RESULTS

Before the development of the SFL technique, the various linearized methods to determine the flow field within the cylindrical cavity were inadequate. Although the primitive assumption for the stretching functions used in reference 1 produced a reasonable value for K, the analysis was in error by as much as 36% when used to obtain a solution for the shear stress at the wall in the UIV problem. This assumption, which is the same as that used by Mills,[4] is that the stretching functions are equal constants given by the reciprocal of the free stream velocity KU. On the other hand, when the stretching functions were assumed such that they correctly predicted the shearing stress for the UIV problem, it was not possible to obtain a reasonable value for K. Moreover, any method which yielded a constant value of the stretching function for the NUIV problem could not be correct, since the dependency of shear stress upon the NUIV distribution must decrease with increasing distance downstream. Unlike other methods, the SFL technique determines the stretching function a priori and should be valid for both NUIV and UIV problems.

Figure 2 compares, over a range of λ, the qualitative solution for $k_{m,s}$ given in reference 1 with the SFL solution for $k_{m,s}$. The values shown are for the end of the moving wall and the end of the stationary wall. The stretching functions for the moving and stationary wall are unequal at all λ. Since the shear stress at the wall is proportional to $\sqrt{k_{m,s}}$, it is easily seen that the qualitative solution for the shear stress will be too high at the end of the stationary wall and too low at the end of the moving wall.

Figure 3 indicates the large variation of $k_{m,s}$ with distance

from the leading edge for $\lambda = 3$. Since the influence of the NUIV distribution decreases downstream, the SFL stretching functions, at large x, approach the SFL stretching functions for the UIV case having the same boundary conditions.

A comparison of the drag on the moving wall determined by the SFL solution with that determined by the qualitative solution is shown in Figure 4 for a range of λ. The qualitative solution yields results which are flow for $\lambda < 2.2$ and high for $\lambda > 2.2$. The Blasius solution for the drag on a flat plate having the same length as the moving wall is also indicated in this figure.

Figure 5 compares the shear stress at the wall given by the SFL solution with that given by the qualitative solution. The largest differences occur at large and at small x. However, the integrated values of $\tau_{m,s}$ for the qualitative solution agree with those for the SFL solution, and the qualitative solution yields a good value for the core velocity ratio, K. Also, Figure 6 indicates that the usual $1/\sqrt{x}$ dependence of the shear stress in the absence of free stream pressure gradients is not realized for NUIV problems. Instead, on the basis of the SFL solution, τ appears to be proportional to $x^{-.58}$ for the moving wall and to $x^{-.65}$ for the stationary wall.

The velocity distributions on the moving and stationary wall are shown in Figures 6a,b for $\lambda = 1$, and in Figures 7a,b for $\lambda = 3$. The SFL solution for the $\lambda = 3$ case can be compared directly with the qualitative solution given in Figures 5a,b of reference 1. The qualitative solution is equivalent to Mills' solution. This comparison indicates that close to the moving wall, the SFL solution has a larger velocity than

the qualitative solution. The largest difference between the solutions occurs at small x.

The following general observations can be made about the flow field predicted by the SFL solution: 1) the BL on the stationary wall is always much thicker than that on the moving wall. This observation might indicate that on the stationary wall diffusion of momentum dominates over convection while on the moving wall, the converse is true. 2) In each of the velocity profiles, the shear stress changes sign as one moves away from the wall. Thus, it appears from the present solution that the oscillatory shear stress at the core is opposed to the shear stress at the wall. 3) A comparison of Figure 6a,b with Figure 7a,b indicates that the BL thickness increases with λ for the same Reynolds number and length of moving wall. This is to be expected since K decreases with increasing λ. 4) Comparing Figure 6a with 6b, or Figure 7a with 7b, one can easily deduce that there is a momentum flux into the core away from the stationary wall and out of the core towards the moving wall.

As discussed in reference 1, the existing experimental results for recirculatory flow fields are questionable. However, the SFL solution is in good agreement with Mills' experimental results.

VALIDITY OF THE SFL SOLUTION

The assessment of the accuracy of the SFL solution for the NUIV problem is difficult without the exact solution in hand. The next best alternative to a complete exact solution is an exact result for some sensitive characteristic of the flow, which may also be evaluated from the SFL solution. The core velocity ratio, K, for which Wood derived an exact result, is one such flow characteristics, and will be used here to assess the validity of the SFL technique. It is expected that any inaccuracy in the velocity distributions will have a large effect on K, since it depends directly on the velocity gradient at the wall.

Before comparing the exact and the SFL results for K, the following comments may be made on the expected accuracy. It has been shown in reference 2 for the UIV case, for which the exact solution is known, that there is less than 3% error in the SFL solution for the wall shear stress with $K/U > .3$. For $K/U < 1$, this error decreases for increasing K. On a stationary wall, the SFL shear stress is shown to be too low, while on a moving wall, the SFL shear stress is shown to be too high. Thus, one would expect that the SFL result for K should be larger than the exact result for K, and that the error between the exact and SFL result would increase for $K \rightarrow 0$. Actually, this limitation is not as significant as it appears, since for $K \rightarrow 0$ several of the other assumptions, particularly the assumption that the core is centered, also begin to break down.

Shown in Figure 8 is a comparison of the SFL and the exact results for K as a function of the order of approximation, p, for the linear velocity distributions on the moving and the stationary walls.

Only five values were chosen for p (p = 0, 1, 2, 3, 4), and these demonstrated that the SFL result for K is rapidly convergent. For $\lambda = 1$, the SFL result for K appears to be asymptotic to a value of .73 (3% high), while for $\lambda = 3$ the K appears to be asymptotic to a value of .55 (10% high). This result is consistent with what is to be expected based on the previous discussion of the UIV analysis.

Another factor which bears on the validity of the solution is the dependence of K on $(F_m + F_s)$, i.e., at $\lambda = 1$ a 1% change in $(F_m + F_s)/F_m$ produces a 2% change in K, while at $\lambda = 3$ a 1% change in $(F_m + F_s)/F_m$ produces a 3% change in K. This factor indicates the sensitivity of K as a measure of the validity of the SFL technique.

The SFL result for K referred to above was determined as part of the numerical analysis in order to assess the accuracy of the SFL solution. Now that this accuracy has been assessed, K may be prescribed by the Wood criterion for the remainder of the computations. This will mean that the shear stress at the wall may be in error by as much as 3%, but it greatly simplifies the numerical analysis.

Thus, the agreement in the exact and the SFL result for K appears to be sufficiently good to provide a check of the SFL technique as a means for the determination of the peripheral BL in a recirculatory flow field.

CONCLUDING DISCUSSION AND SUGGESTIONS FOR FUTURE WORK

The SFL technique is shown in reference 2 to yield valid results for the UIV case by direct comparison with the exact solution. The SFL technique is shown in the present paper to yield valid results for the flow field in a circular cavity, by direct comparison of the SFL result for the core velocity ratio, K, with an exact result for K. Based on these results, it would seem that the SFL technique may with confidence be applied to more general BL problems.

The success of this technique suggests the following items of future work:

1) better experimental data should be obtained for the flow in a cylindrical cavity,

2) the effect of using different criteria to derive $k(x)$ should be studied,

3) rigorous error bounds should be determined for the SFL solution, and

4) the applicability of the SFL technique to other nonlinear partial differential equations should be studied.

APPENDIX I

NUMERICAL COMPUTATION

The numerical computations were performed at the RPI Computer Laboratory on an IBM 360/50 using a FORTRAN compiler. For a third order solution (p = 2) the stretching functions and velocity distributions could be obtained in approximately 5 minutes of computation time if optimized coding is used. The calculation procedure may be summarized as follows:

1) A value $\overset{(o)}{K}$ is assumed for the core velocity ratio.

2) The constants $\overset{(o)}{k}_{m,s}$ are assumed for the stretching functions,

3) The values $\hat{a}^{(o)}$, $\hat{c}^{(o)}$ and the functions $\overset{(o)}{g}_{m,s}(x)$ are computed from equations 5c and 3.

4) The velocity distributions $\hat{u}_{m,s}(\hat{x}_{m,s}, \psi)$ are determined from equations 5a,b.

5) The functions $\epsilon^{(o)}{}_{m,s}(\hat{x}_{m,s}, \hat{a}^{(o)}, \hat{c}^{(o)})$ are determined from equation 7.

6) Higher order approximations for the stretching-functions $k_{m,s}(x)$ are calculated from equation 8b, i.e.,

$$\overset{(1)}{k}(x) = \overset{(o)}{\epsilon}_{m,s}\left(\overset{(o)}{g}_{m,s}(x), \overset{o}{\hat{a}}, \overset{o}{\hat{c}}\right)$$

7) Higher order approximations $\overset{!}{\hat{a}}$, $\overset{!}{\hat{c}}$ and $\overset{(1)}{g}_{m,s}(x)$ are calculated from equations 5c and 3.

8) Steps 2 through 7 are then repeated until the absolute relative error in $\hat{a}$ and $\hat{c}$ is less than 1%, i.e., until

$$\left| \overset{(n+1)}{\hat{a}} - \overset{(n)}{\hat{a}} \right| \leq 0.01 \overset{(n+1)}{\hat{a}}$$

and

$$\left| \hat{c}^{(n+1)} - \hat{c}^{(n)} \right| \leq 0.01\, \hat{c}^{(n+1)}$$

Usually only n = 3 was required to achieve this result.

9) With the required accuracy in $\hat{a}$, $\hat{c}$ and $g_{m,s}$ obtained, the sum of the drag on the moving wall, F_m, and on the stationary wall, F_s, is calculated in the physical plane. If the absolute relative error in $(F_m + F_s)$ is less than 0.2%, i.e., if

$$\left| F_m + F_s \right| \leq 0.002\, F_m$$

then the value $K^{(o)}$ was assumed correctly. If not, steps 1 through 9 were repeated with a different K until this condition was met. Because of the linearity of $(F_m + F_s)$ with K, the correct value of K could usually be chosen in the third guess. The overall numerical accuracy for each of F_m and F_s is expected to be $\pm$ 2%.

REFERENCES

1. Ernst, W.D., "Recirculatory Flow in a Cylindrical Cavity," Rensselaer Polytechnic Institute Tech. Report TR PT 6804, 1968.

2. Ernst, W.D., "Linearized Flow Past a Flat Plate," Rensselaer Polytechnic Institute Tech. Report TR PT 6901, 1969.

3. Wood, W.W., "Boundary Layers Whose Streamlines are Closed," J. Fluid Mech. 2, p. 77, 1957.

4. Mills, R.D., "On the Closed Motion of a Fluid in a Square Cavity," J. Roy. Aero. Soc. 69, p. 116, 1965.

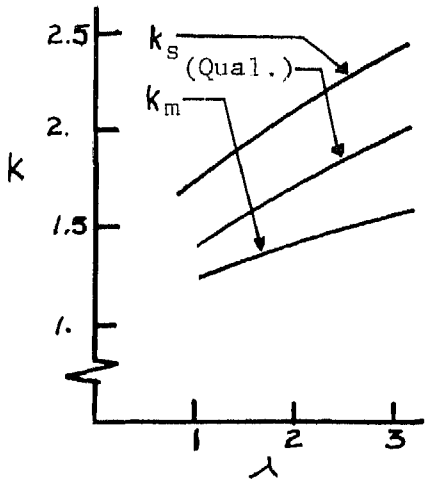

Fig. 2
Stretching Functions
at End of Wall

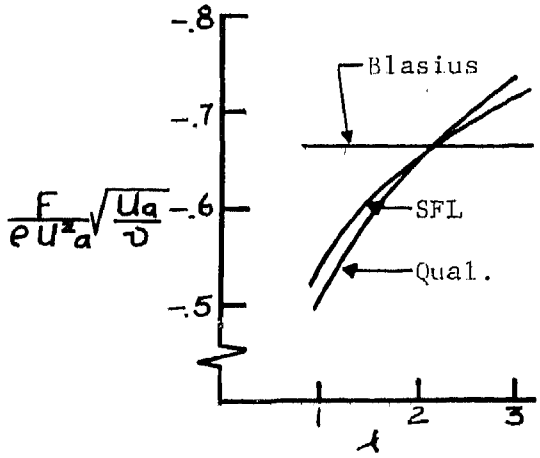

Fig. 4
Drag on Moving Wall

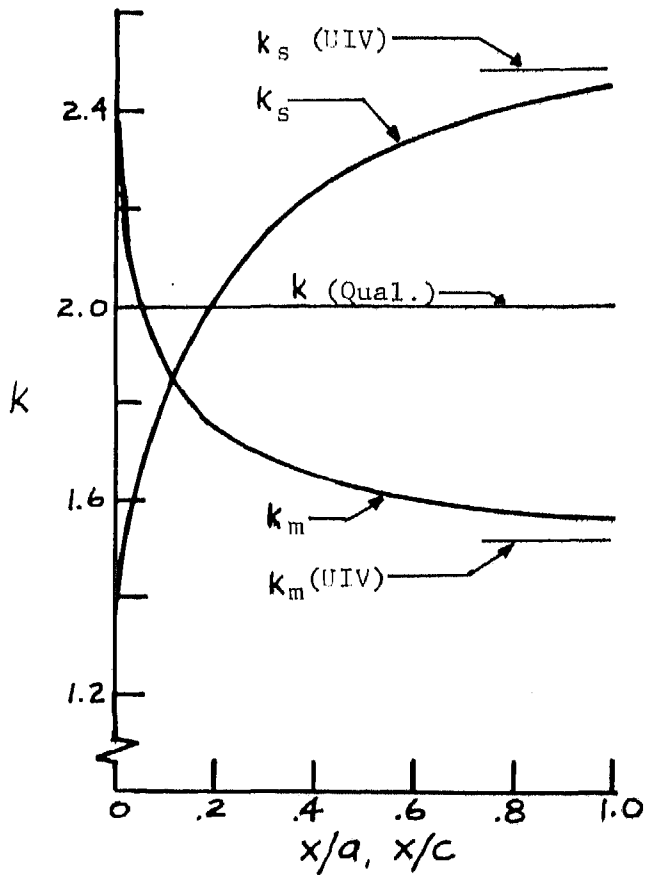

Fig. 3
Stretching Functions for $\lambda = 3$

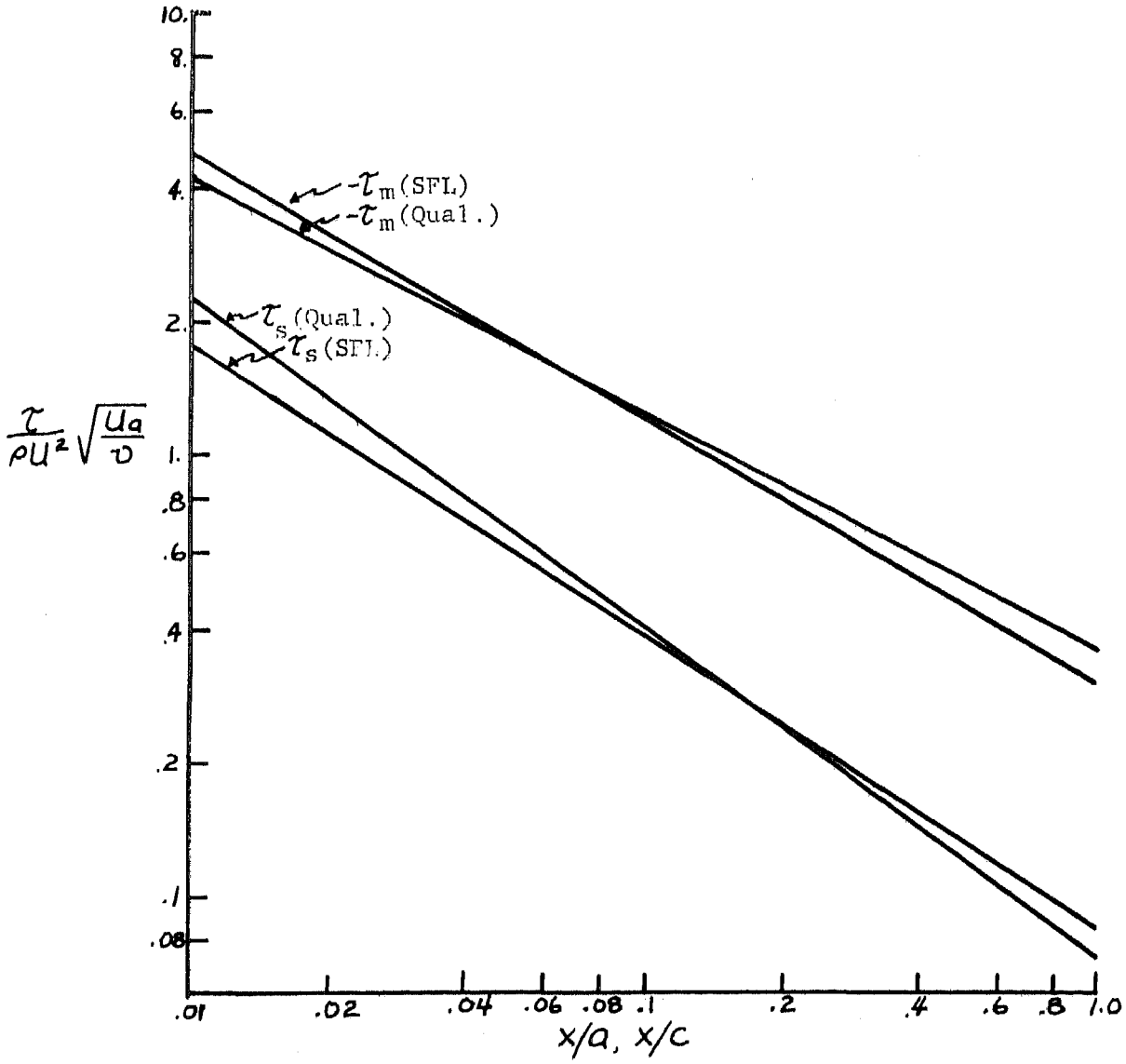

Fig. 5
Wall Shear Stress Variation for $\lambda = 3$

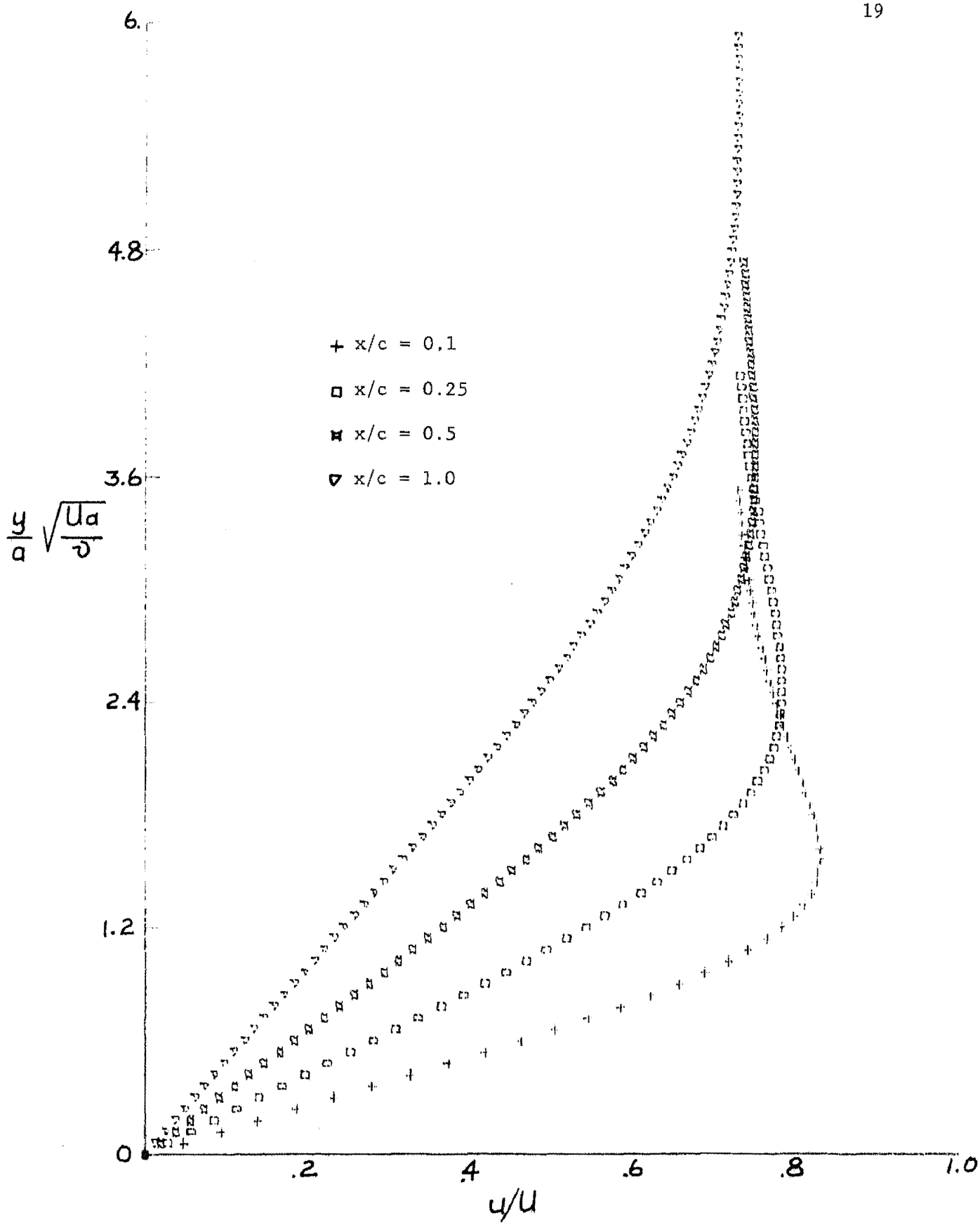

Fig. 6a
SFL Boundary Layer Velocity Profiles on Stationary Wall for $\lambda = 1$

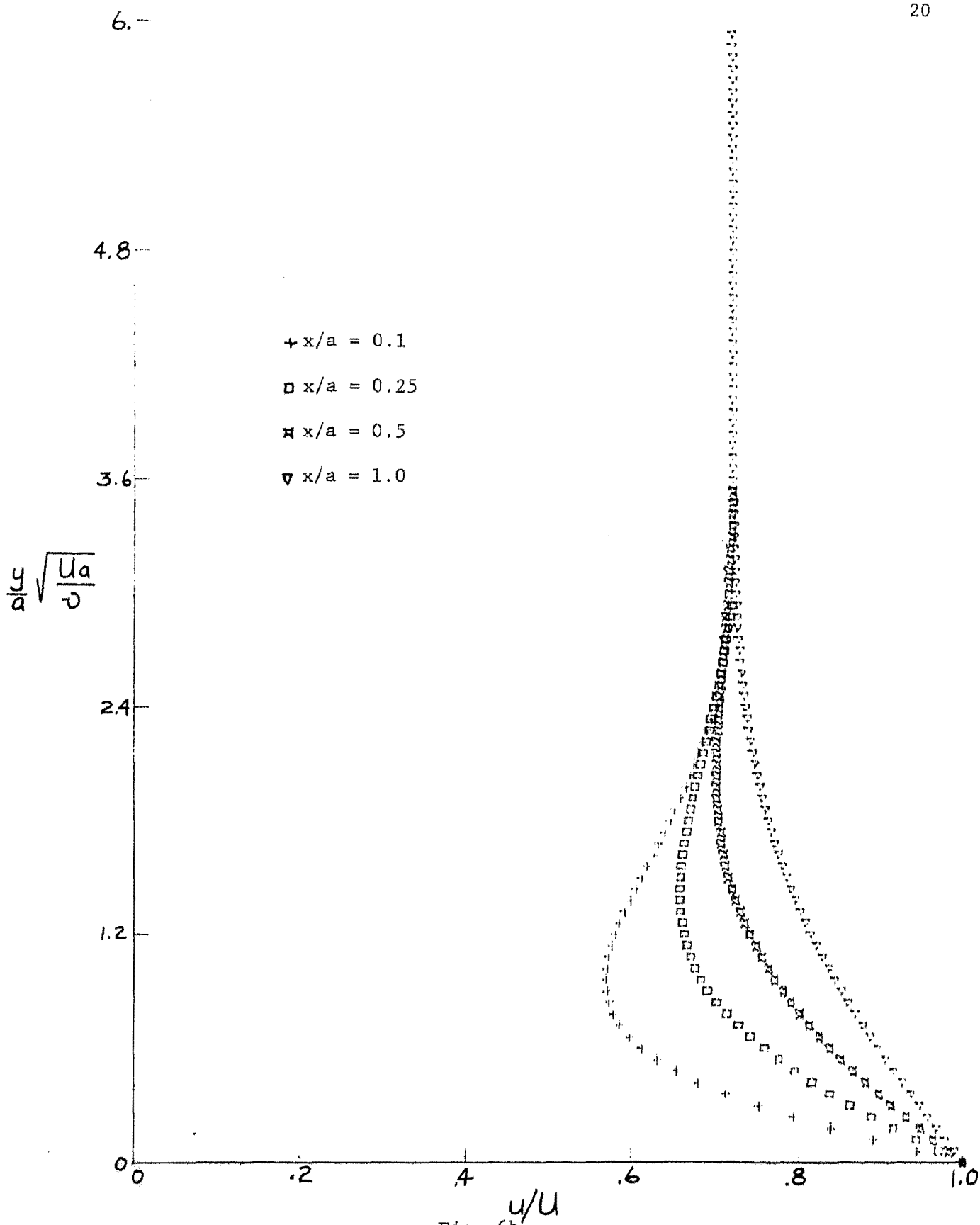

Fig. 6b
SFL Boundary Layer Velocity Profiles on Moving Wall for $\lambda = 1$

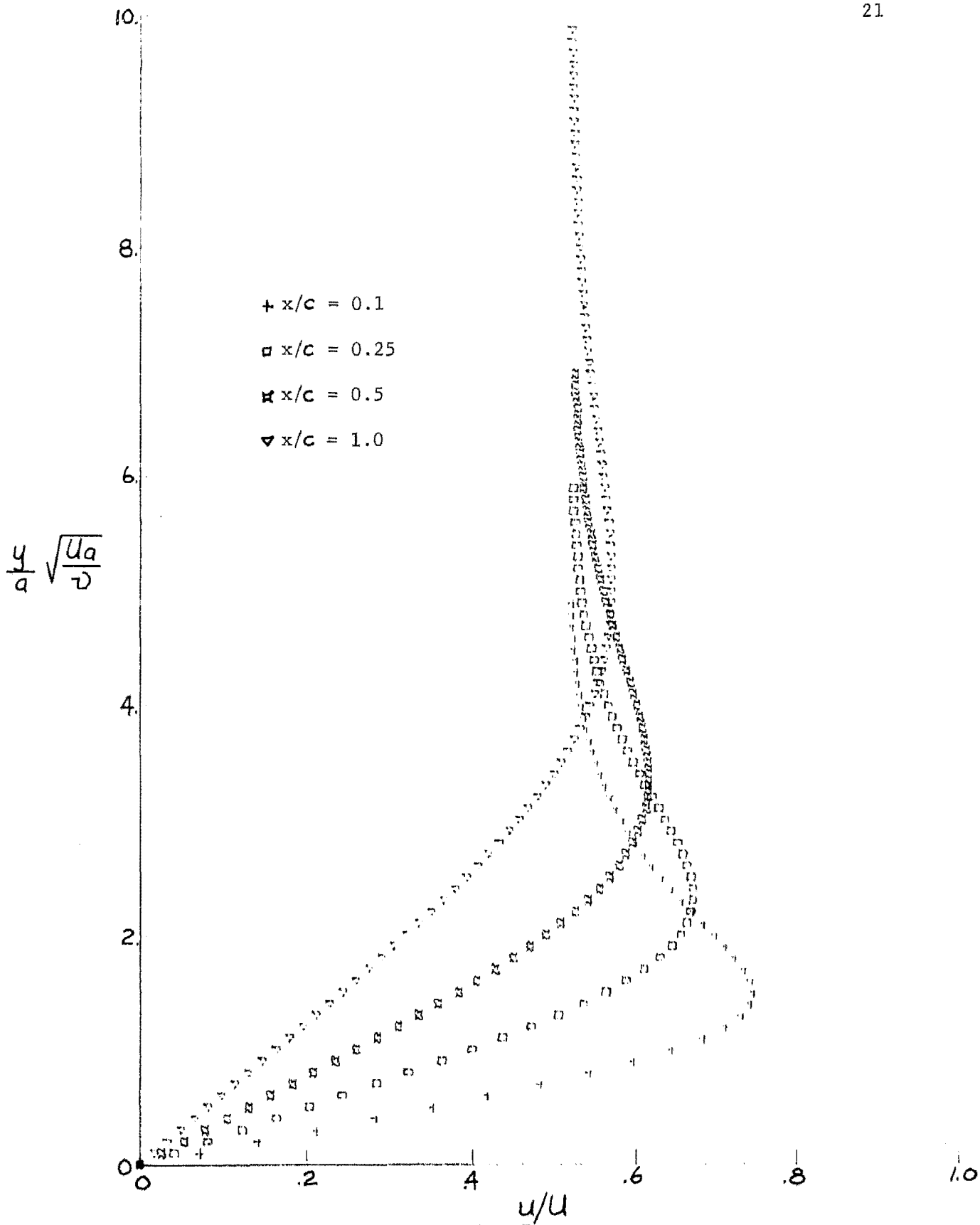

Fig. 7a
SFL Boundary Layer Velocity Profiles on Stationary Wall
for $\lambda = 3$

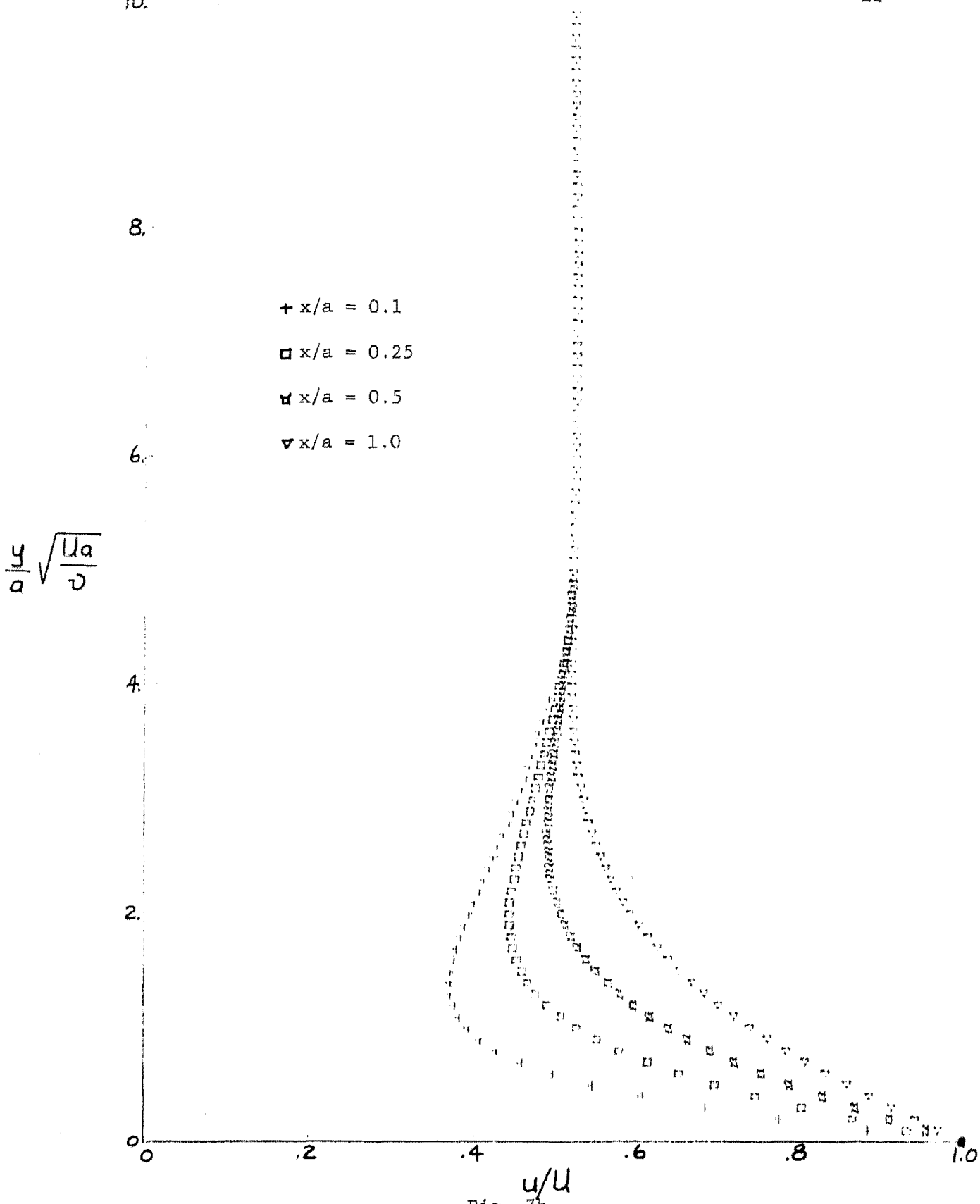

Fig. 7b
SFL Boundary Layer Velocity Profiles on Moving Wall for $\lambda = 3$

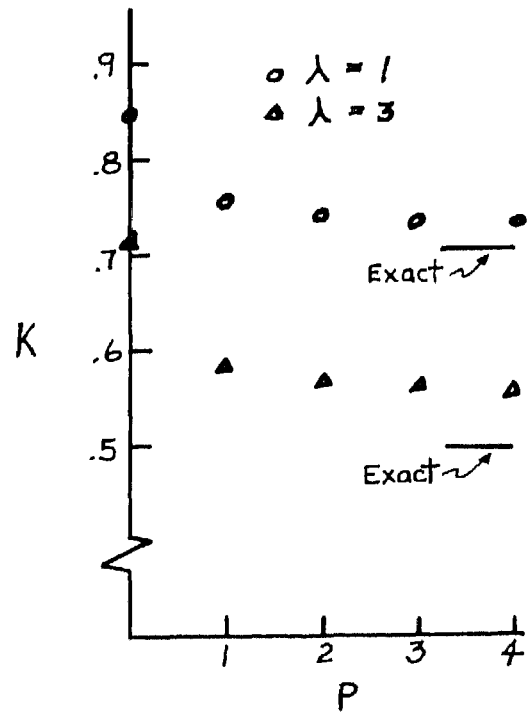

Fig. 8
Convergence of the
Core Velocity Ratio